Alberto Carpinteri
Erica Cadamuro
Mauro Corrado*

DOI: 10.1002/suco.201300056

Minimum flexural reinforcement in rectangular and T-section concrete beams

The prescriptions provided by codes of practice for assessing the minimum reinforcement amount for strength purposes in reinforced concrete beams usually disregard the non-linear contribution of concrete in tension and size-scale effects. In the present paper, these phenomena are taken into account correctly in the description of the flexural failure in lightly reinforced concrete beams by means of a numerical algorithm based on non-linear fracture mechanics. In this context, the application of dimensional analysis permits a reduction in the number of governing parameters. In particular, it is demonstrated analytically that only two dimensionless parameters, referred to as reinforcement brittleness number and stress brittleness number, are responsible for the brittle-to-ductile transition in the mechanical response. According to this approach, new formulae suitable for evaluating the minimum reinforcement in practical applications is proposed for both rectangular and T-sections. A comparison with experimental results demonstrates the effectiveness of the proposed model for different reinforcement percentages and beam depths.

Keywords: reinforced concrete, code provisions, minimum reinforcement, dimensional analysis, size effects, cohesive crack

1 Introduction

The minimum reinforcement amount in concrete elements is usually determined by two different requirements: limiting crack width in the serviceability limit state conditions and avoiding the hyper-strength phenomenon. As regards crack control, this is required for different reasons, such as appearance, imperviousness and durability [1]. From the point of view of durability, for instance, cracks in the concrete cover may lead to the ingress of various agents (e.g. oxygen, water and chlorides), which may in turn lead to the onset and propagation of corrosion of the steel reinforcement. These requirements are usually satisfied by limiting the crack width to levels specified by standards (see, for instance, sections 7.6.3 to 7.6.5 in *fib* Model Code for Concrete Structures 2010 [2]). Since crack opening is a function of the tensile stress in the rebars, among other parameters, the upper limits to crack width become lower limits for the area of steel reinforcement. On the other hand, the hyper-strength phenomenon is avoided by imposing that the maximum cracking load is lower than the ultimate load, given by the reaction of the yielded reinforcement multiplied by the moment arm. For this purpose, several formulae are provided by different standards, although most of them are too simplistic. The present paper focuses on the strength criterion, with particular emphasis on the issue of size effects, which are currently disregarded by the standards.

1.1 Code provisions

Limit analysis of reinforced concrete (RC) beams usually disregards the non-linear contribution of concrete in tension in the evaluation of the load-carrying capacity. This assumption does not always lead to a safe design condition, e.g. in the case of flexural members that – for architectural or other reasons – have a larger cross-section than that required for strength. With a very small amount of tensile reinforcement, the tensile concrete strength in fact makes a substantial contribution to the definition of the peak cracking load, which may turn out to be higher than the ultimate load. In this case a sudden drop in the load-carrying capacity takes place, from the value of the maximum cracking load to the ultimate load (hyper-strength phenomenon). This behaviour is characterized by unstable crack propagation, with a decrease in the fracture moment while the crack extends. For this reason, all national and international codes of practice impose limitations on the minimum reinforcement amount in order to prevent sudden failure. Most of them consider only two parameters: concrete grade and steel yield strength, whereas the effects of other important parameters, e.g. beam depth, are completely neglected. According to the approach of the ACI 318 Building Code [3, 4], the condition of minimum reinforcement is defined by the equality $\phi M_u = M_{cr}$, where ϕ is a resistance factor, assumed to be 0.9, M_u is the nominal flexural resistance (or ultimate load) given by the reaction of the yielded reinforcement times the moment arm, and M_{cr} is the cracking moment of the plain concrete section evaluated on the basis of the flexural tensile strength $f_{ct,fl}$. By means of simple substitutions and some analytical manipulations (see *Seguirant* et al. [5] for more details), the value for the minimum reinforcement area can be expressed thus:

* Corresponding author: mauro.corrado@polito.it

Submitted for review: 19 July 2013
Revised: 2 January 2014
Accepted for publication: 29 January 2014

$$A_{\mathrm{s,min}} = \frac{K}{12}\frac{\sqrt{f_{\mathrm{ck}}(\mathrm{MPa})}}{f_{\mathrm{yk}}} b_{\mathrm{w}} d(\mathrm{mm}^2) \quad (1)$$

where:

$$K = 7.5\left(\frac{h}{d}\right)^2\left(\frac{C}{5.1}\right) \quad (2)$$

C multiplier to adjust section modulus for different beam shapes
f_{ck} characteristic compressive strength of concrete
f_{yk} yield strength of steel
b_{w} width of beam
h overall depth of beam
d effective depth of beam

For T-beams with the flange in compression, using a value $C = 1.5$ (it is 1.0 for rectangular members), and $h/d = 1.2$, parameter K assumes a value slightly larger than 3. Therefore, the expression adopted in ACI 318-95 [3], and still included in ACI 318-08 [4], is

$$A_{\mathrm{s,min}} = 0.25\frac{\sqrt{f_{\mathrm{ck}}(\mathrm{MPa})}}{f_{\mathrm{yk}}} b_{\mathrm{w}} d(\mathrm{mm}^2) \geq 1.4\frac{b_{\mathrm{w}} d}{f_{\mathrm{yk}}}(\mathrm{mm}^2) \quad (3)$$

The expression provided by the 2004 Eurocode 2 [6] and *fib* Model Code 2010 [2] has a similar derivation. The relation proposed for both rectangular and T-beams is based on the average uniaxial tensile strength of concrete f_{ctm} instead of the flexural tensile strength $f_{\mathrm{ct,fl}}$:

$$A_{\mathrm{s,min}} = 0.26\frac{f_{\mathrm{ctm}}}{f_{\mathrm{yk}}} b_{\mathrm{w}} d \geq 0.0013 b_{\mathrm{w}} d \quad (4)$$

It is worth noting that the coefficient 0.26 in Eq. (4) is derived by assuming a ratio $h/d = 1.2$ and a resistance factor $\phi = 0.9$.

Only the Norwegian Standard NS 3473 E [7] accounts for the effect of member size. The reinforcement should have a total cross-sectional area equal to

$$A_{\mathrm{s,min}} = 0.35 k_w A_{\mathrm{c}} f_{\mathrm{ctk,0.05}} / f_{\mathrm{yk}} \quad (5)$$

where $f_{\mathrm{ctk,0.05}}$ is the lower characteristic tensile strength of concrete and A_{c} is the gross cross-sectional area. The size effects are taken into account by means of factor k_w, equal to $1.5 - h/h_1 \geq 1$, where h is the beam depth in m and $h_1 = 1.0$ m. In this case only rectangular members are considered.

1.2 Models for computing minimum reinforcement

From the modelling point of view, significant contributions to the evaluation of the minimum flexural reinforcement were derived from the application of the **bridged crack model** [8, 9] – an approach based on linear elastic fracture mechanics (LEFM) – to the study of crack propagation in the presence of reinforcement. More precisely, the model considers an RC beam element characterized by a rectangular cross-section with a layer of steel reinforcement and an edge crack. The stress intensity factor at the crack tip K_{I} is a function of the externally applied bending moment and the reinforcement reaction by means of suitable shape functions. The cracking moment is obtained when K_{I} reaches its critical value K_{IC}, and the corresponding reinforcement reaction is determined by setting a kinematical compatibility condition on the crack opening (crack opening displacement equal to zero before steel yielding). Both of these are functions of the relative crack length. According to the analytical formulation of the bridged crack model, the overall behaviour is only a function of the **reinforcement brittleness number** N_P, defined on the basis of the mechanical and geometrical parameters [8]:

$$N_P = \frac{A_{\mathrm{s}}}{b_{\mathrm{w}} h}\frac{f_{\mathrm{yk}} h^{0.5}}{K_{\mathrm{IC}}} \quad (6)$$

where:
f_{yk} steel yield strength
b_{w} width of beam
h overall depth of beam
K_{IC} concrete fracture toughness
A_{s} area of tension reinforcement

Although originally defined as a "brittleness number", N_P represents a ductility parameter: the larger its value, the more ductile is the mechanical behaviour. In particular, the yielding and the ultimate bending moments are increasing functions of N_P. Therefore, a brittle response, with a softening branch after the peak cracking load, is expected for low values of N_P, whereas by increasing its value (it typically ranges from 0.1 to 10), a ductile response is predicted, with a hardening behaviour after the cracking load and a large inelastic displacement due to steel yielding. However, it is worth noting that by increasing N_P beyond an upper limit value, which is a function of the structural scale, the overall response becomes brittle again due to the appearance of a crushing collapse before steel yielding. As far as the minimum reinforcement amount is concerned, it is possible to define N_{PC} as the critical value separating the brittle response from the ductile one. The following empirical equation has been proposed by *Bosco* and *Carpinteri* [10, 11] to express the dependence of N_{PC} on the average concrete compressive strength f_{cm}:

$$N_{PC} = 0.1 + 0.0023 f_{\mathrm{cm}} \quad (7)$$

According to Eq. (7), higher values of N_{PC} are obtained by increasing the concrete compressive strength. The formula for the minimum reinforcement area can be obtained by matching the expression of N_P (Eq. (6)) to that of N_{PC} (Eq. (7)) and solving for A_{s}:

$$A_{\mathrm{s,min}} = \frac{K_{\mathrm{IC}}}{f_{\mathrm{yk}}}\left(0.1 + 0.0023 f_{\mathrm{cm}}\right) b_{\mathrm{w}} h^{0.5} \quad (8)$$

Eq. (8) reveals how $A_{\mathrm{s,min}}$ depends on the mechanical and geometrical properties. In particular, it is proportional to the square root of the beam depth h.

Several other models have been proposed for evaluating the minimum reinforcement amount. Most of them reveal a decrease in the minimum amount by increasing the size scale, although there is a large variation in the results. This is mainly due to the different definitions assumed for the minimum reinforcement as well as the different approaches used to tackle the problem. *Hawkins* and *Hjorteset* [12], for instance, studied the problem with the cohesive crack model, and proposed an expression for the minimum reinforcement on the basis of a size-dependent nominal flexural tensile strength of concrete. *Gerstle* et al. [13] proposed an analytical formula obtained by considering the equilibrium of tensile and compressive forces and the deformation of concrete. They defined the minimum reinforcement amount as the quantity below which crack propagation becomes unstable, i.e. the moment versus crack length curve assumes a decreasing trend. *Ruiz* et al. [14] evaluated $A_{s,min}$ taking into account the bond-slip behaviour between concrete and steel along the transfer length and by adopting the cohesive crack model to describe the fracture propagation. Finally, *Appa Rao* et al. [15] proposed an approach based on LEFM concepts, using the two-parameter fracture model proposed by *Jenq* and *Shah* [16] for concrete. All the formulae obtained by the aforementioned models are given in Table 1, with details of the parameters involved.

In the present paper, the problem of the minimum reinforcement amount is analysed by means of a numerical approach based on non-linear fracture mechanics [17]. First, its effectiveness is proved by a comparison between numerical simulations and the results of an experimental campaign involving three-point bending tests on RC beams. A parametric analysis is then carried out in order to evaluate the minimum reinforcement amount by varying concrete grade and beam size. Finally, **dimensional analysis** is applied in order to combine the different variables characterizing the phenomenon into a reduced number of governing parameters (N_P and s). As a consequence, the results of the parametric analysis align perfectly along a hyperbolic curve in the diagram N_{PC} vs. s, making the definition of a new design formula easier, based on the results of the numerical simulations. With respect to the formulae available in the literature, the one proposed is very synthetic and suitable for practical purposes without gross simplifications of the set of variables governing the problem.

2 Analytical and numerical investigation

2.1 Integrated cohesive/overlapping crack model

Let us consider a reinforced concrete beam element with a rectangular cross-section of width b_w, depth h, and effective depth d. The beam segment has a length l equal to its depth and is subjected to the external bending moment M. The middle cross-section is representative of the mechanical behaviour of the whole element, since all the non-lin-

Table 1. Minimum reinforcement according to different models [11–15]

Authors	Model formula
Bosco and *Carpinteri* [11] (1992)	$A_{s,min} = \frac{K_{IC}}{f_{yk} h^{0.5}}\left(0.1 + 0.0023 f_{cm}\right) b_w h$
Hawkins and *Hjorteset* [12] (1992)	$A_{s,min} = 0.175\left(\frac{f_f}{f_{ctm}}\right)\left(\frac{f_{ctm}}{f_{yk}}\right)\left(\frac{h}{d}\right) b_w h$
Gerstle et al. [13] (1992)	$A_{s,min} = \frac{E_c}{E_s}\left(\sqrt{0.0081 + 0.0148 f_{ctm} h / E_c w_c} - 0.0900\right)^{1/2} b_w h$
Ruiz et al. [14] (1999)	$A_{s,min} = \frac{0.174}{1-\gamma} \; \frac{1 + (0.85 + 2.3\beta_1)^{-1}}{f_y^* - \eta_1 \varphi} b_w h$ where: $\beta_1 = h/(\alpha\, l_{ch})$; $l_{ch} = E_c \mathcal{G}_F / f_{ctm}^2$; $\alpha = (65 + 15\, d_{max}/d_0)/170$; $d_0 = 8$ mm; d_{max} = maximum aggregate size; $\gamma = c/h$; $f_y^* = f_{yk}/f_{ctm}$; $\eta_1 = 15$, $\varphi = (\beta_1^{0.25} - 3.61\,\gamma_1) \geq 0$.
Appa Rao et al. [15] (2007)	$A_{s,min} = \left(-0.01 + \frac{40.10}{d}\right)\frac{f_{ck}^{1.14}}{f_{yk}^{0.57}} b_w d$

$A_{s,min}$	minimum steel area	K_{IC}	concrete fracture toughness
d	effective beam depth	h	overall beam depth
E_c	concrete elastic modulus	f_{ctm}	average concrete uniaxial tensile strength
f_{yk}	steel yield strength	f_{cm}	average concrete compressive strength
E_s	steel elastic modulus	ρ_{min}	minimum steel percentage
w_c	critical crack width	c	reinforcement cover
$\mathcal{G}_F$	concrete fracture energy	b_w	beam width
f_f	concrete flexural tensile strength (size-dependent)		

earities, i.e. concrete cracking in tension, steel yielding and crushing of concrete in compression, are localized in this section, whereas the outer parts exhibit an elastic response. The numerical model proposed here to describe the fracture behaviour of lightly reinforced RC beams is derived by the more general algorithm introduced by *Carpinteri* et al. [17] for modelling the mechanical response of all the possible situations ranging from plain to over-reinforced concrete beams. It is based on a numerical procedure similar to those proposed by *Carpinteri* [18] and *Planas* and *Elices* [19] for implementing a cohesive crack.

2.2 Constitutive models

The mechanical response of concrete in tension is described by the **cohesive crack model** [18, 20], which considers a damaged and microcracked process zone ahead of the real crack tip, partially stitched by inclusions, aggregates or fibres, where non-linear and dissipative phenomena take place. A linear-elastic stress-strain relationship is assumed for the undamaged phase (see Fig. 1a), whereas a softening stress-crack width relationship describes the process zone up to the critical opening w_{cr}^{t} being reached (see Fig. 1b). The softening function $\sigma = f(w)$ is a material property, likewise the uniaxial tensile strength f_{ctm}, the critical value of the crack opening w_{cr}^{t} and the fracture energy $\mathcal{G}_F$. The shape of $f(w)$ may vary from linear to bilinear or even more complicated relationships depending on the characteristics of the material considered and the problem being analysed. For instance, when plain concrete subjected to a high strain gradient is being studied, a simple linear softening law can be sufficient to obtain accurate results. On the other hand, bilinear relationships with long tails are necessary to describe fibre-reinforced concrete elements, taking into account the closing tractions exerted by fibres for large crack opening values.

As far as modelling concrete crushing failure is concerned, the **overlapping crack model** introduced by *Carpinteri* et al. [17, 21] is adopted. According to such an approach, the inelastic deformation in the post-peak regime is described by a fictitious interpenetration of the material, while the remaining part of the specimen undergoes an elastic unloading. Therefore, a pair of constitutive laws is considered, in close analogy with the cohesive crack model: a stress-strain relationship until the compressive strength is achieved, and a stress-displacement (i.e. overlapping) relationship describing the phenomenon of concrete crushing. The latter law, usually assumed as a linear decreasing function, describes how the stress in the damaged material decreases from its maximum value down to zero as the fictitious interpenetration increases from zero to the critical value w_{cr}^{c}. The crushing energy $\mathcal{G}_C$, which is a dissipated surface energy defined as the area beneath the post-peak softening curve, can be assumed as a true material property since it is almost independent of the structural size.

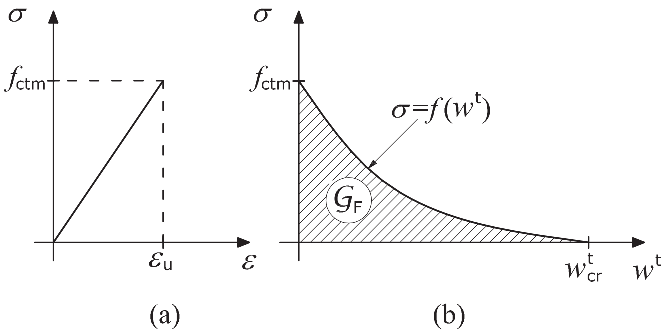

Fig. 1. Cohesive crack model: a) linear-elastic σ–ε law, and b) post-peak softening σ–*w* relationship

The interaction between steel and concrete along the rebar is not modelled specifically. The reinforcement reaction is included in the numerical algorithm proposed in the next section as an external applied force, function of the crack opening displacement according to a suitable constitutive law. On the basis of the bond-slip relationship provided by *fib* Model Code 2010 [5], and by imposing equilibrium and compatibility conditions, it is possible to correlate the reinforcement reaction to the relative slip at the crack edge, which corresponds to half the crack opening displacement. Typically, the relationship obtained is characterized by an ascending branch up to steel yielding, corresponding to which there is a critical value of the crack opening w_y. After that, the steel reaction is nearly constant. It has been shown that the value of w_y varies in the range 0.1–0.5 mm depending on steel amount, rebar diameter and number of rebars (see also [22]). In the present study, a value of 0.2 mm has been assumed, more consistent with the small reinforcement percentages considered. However, it is worth noting that this parameter has a limited effect on the evaluation of the minimum reinforcement amount since it barely affects the maximum cracking load M_{cr}. In the present algorithm, this stress-displacement law is introduced in the input together with the cohesive and overlapping constitutive laws.

2.3 Numerical algorithm

The mid-span cross-section of the element shown in Fig. 2a is subdivided into n nodes, where cohesive and overlapping stresses are replaced by equivalent nodal forces F_i which depend on the corresponding relative nodal displacements according to the cohesive or overlapping post-peak laws (Fig. 2a). These horizontal forces can be computed as follows:

$$\{F\} = [K_w]\{w\} + \{K_M\}\, M \tag{9}$$

where:

- $\{F\}$ vector of nodal forces
- $[K_w]$ matrix of coefficients of influence for nodal displacements
- $\{w\}$ vector of nodal displacements
- $\{K_M\}$ vector of coefficients of influence for applied moment M

Eq. (9) permits the fracture and crushing phenomena to be studied by taking into account the elastic behaviour of the RC member. To this end, all the elastic coefficients are computed a priori using a finite element analysis. For symmetry, only a half-element is discretized through quadrilateral plane stress elements with uniform nodal spacing. Horizontal constraints are then applied at the nodes along

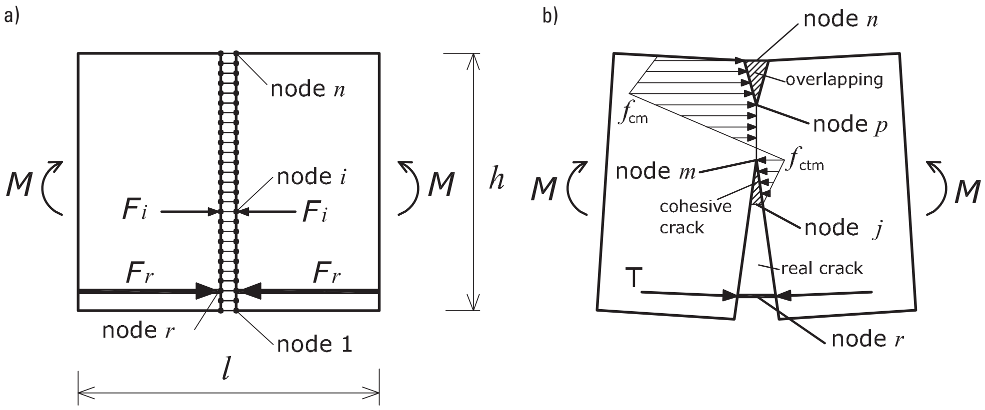

Fig. 2. Scheme of the mid-span cross-section: a) finite element nodes and b) force distribution with cohesive crack in tension, crushing in compression and reinforcement closing forces

the vertical symmetry edge. Each coefficient of influence $K_w^{i,j}$, which relates the nodal force F_i to the nodal displacement w_j, is computed by imposing a unitary displacement on the corresponding constrained node. On the other hand, the coefficients K_M^i are computed by imposing a unitary external bending moment.

In the generic situation shown in Fig. 2b, the following equations can be considered, taking into account, respectively, the stress-free crack (Eq. (10a)), the cohesive softening law (Eq. (10b)), the steel constitutive law (Eq. (10c)), the undamaged zone (Eq. (10d)) and the overlapping softening law (Eq. (10e)):

$$F_i = 0;\ \text{for i} = 1, 2, \ldots, (j-1);\ \text{i} \neq r \tag{10a}$$

$$F_i = f(w_i);\ \text{for i} = j, \ldots, (m-1);\ \text{i} \neq r \tag{10b}$$

$$F_i = h(w_\text{i});\ \text{for i} = r \tag{10c}$$

$$w_i = 0;\ \text{for i} = m, \ldots, p \tag{10d}$$

$$F_\text{i} = g(w_\text{i});\ \text{for i} = (p+1), \ldots, n \tag{10e}$$

where:
- j real crack tip
- m fictitious crack tip
- p fictitious overlapping zone tip
- r reinforcement layer level

Eqs. (9) and (10) constitute a linear algebraic system of $(2n)$ equations in $(2n+1)$ unknowns, namely $\{F\}$, $\{w\}$ and M. As regards the compatibility requirement between steel and concrete, the displacement of the rebars and that of the surrounding concrete are assumed to be equal. On the other hand, the necessary additional equation derives from the strength criterion adopted to govern the propagation processes. We can set either the force in the fictitious crack tip m, equal to the ultimate tensile force F_u, or the force in the fictitious crushing zone tip p, equal to the ultimate compressive force F_c. It is important to note that cracking and crushing phenomena are physically independent of each other. As a result, the situation that is closer to one of these two possible conditions is chosen to establish the prevailing phenomenon. The driving parameter in the process is the position of the fictitious tip that has reached the limit resistance in the step considered. Only this tip is moved to the next node when passing to the next step. The localized rotation ϑ is computed as follows:

$$\vartheta = \{D_w\}^\text{T}\{w\} + D_M M \tag{11}$$

where $\{D_w\}$ is the vector of the coefficient of influence for the nodal displacements and D_M is the coefficient of influence for the applied bending moment M.

As the present study relates to the analysis of beams of different sizes, it should be noted that the elastic coefficients in Eqs. (9) and (11) are connected to the structural dimension by simple relations of proportionality. Therefore, it is not necessary to repeat the finite element analysis for any different beam sizes considered.

2.4 Application of dimensional analysis to lightly reinforced RC members

When the flexural behaviour of RC beams is studied, then according to the numerical model proposed in the previous section, the functional relationship among the quantities characterizing the phenomenon is

$$M = g\left(f_\text{ctm}, \mathcal{G}_\text{F}, f_\text{ck}, \mathcal{G}_\text{C}, E_\text{c}, f_\text{yk}, A_\text{s}, h; \frac{b_\text{w}}{h}, \frac{l}{h}, \vartheta\right) \tag{12}$$

where:
- M resistant bending moment
- f_ctm average uniaxial tensile strength
- $\mathcal{G}_\text{F}$ fracture energy
- f_ck characteristic compressive strength
- $\mathcal{G}_\text{C}$ crushing energy
- E_c elastic modulus of concrete
- f_yk yield strength of tension reinforcement
- A_s area of tension reinforcement
- h beam depth
- ϑ local rotation of the element

and b_w/h and l/h define the geometry of the sample.

Since we are interested in the mechanical response of lightly reinforced RC beams, the set of variables can be reduced as follows:

$$M = g\left(f_\text{ctm}, \mathcal{G}_\text{F}, E_\text{c}, f_\text{yk}, A_\text{s}, h; \vartheta\right) \tag{13}$$

where the parameters describing the behaviour of concrete in compression, f_{ck} and $\mathcal{G}_C$, are not explicitly considered since the crushing failure is not involved in the failure mechanism. On the other hand, the geometrical ratios of the samples, b_w/h and l/h, are cancelled out since they are assumed to be constant. This assumption permits an investigation of the size-scale effects (all the beam dimensions vary with beam depth), whereas the effects of width and slenderness are not taken into account. The application of *Buckingham*'s Π-Theorem [23] for physical similitude and scale modelling permits a minimization of the dimension space of the primary variables by combining them into dimensionless groups as follows:

$$\frac{M}{h^{2.5}\sqrt{\mathcal{G}_F E_c}} = g_1\left(\frac{f_{ctm}h^{0.5}}{\sqrt{\mathcal{G}_F E_c}}, \frac{A_s}{b_w h}\frac{f_{yk}h^{0.5}}{\sqrt{\mathcal{G}_F E_c}}, \vartheta\frac{E_c h^{0.5}}{\sqrt{\mathcal{G}_F E_c}}\right) \tag{14}$$

if the beam depth h and the concrete fracture toughness $\sqrt{\mathcal{G}_F E_c} = K_{IC}$ are assumed to be the dimensionally independent variables. As a consequence, the dimensionless functional relation for the proposed model becomes

$$\tilde{M} = g_2\,(s, N_P, \vartheta_n) \tag{15}$$

where:

$$s = \frac{K_{IC}}{f_{ctm}h^{0.5}} \tag{16}$$

and N_P, defined in Eq. (6), are the governing dimensionless numbers, $\tilde{M}$ is the dimensionless bending moment and ϑ_n is the normalized local rotation. It is worth noting that the presence of cohesive closing stresses along the fictitious process zone, in addition to a steel reinforcement layer, means that the structural response is governed by two dimensionless numbers instead of only N_P, as in the case of the bridged crack model. In particular, the matrix strength and toughness are considered by the **stress brittleness number** s introduced by *Carpinteri* [24]. In particular, the cracking load is a decreasing function of the dimensionless number s. Therefore, for a fixed value of N_P, by increasing the value of s (it typically ranges from 0.2 to 3.0), the response becomes more and more stable. In general, a transition from brittle to ductile response is obtained by increasing N_P and/or s (a detailed analysis of the transitions ruled by N_P and s is reported in [25]). Physical similarity in the dimensionless moment vs. normalized rotation diagrams is obtained when both N_P and s are kept constant.

3 Comparison of predictions and experimental results

The experimental investigation considered here was carried out by *Bosco* et al. [10, 12] in 1990 with the purpose of verifying the existence of size effects in the flexural behaviour of RC beams. To this end, three-point bending tests were performed on initially unnotched and uncracked reinforced and plain concrete rectangular beams varying in depth from 100 to 800 mm. The effective depth d was set to 0.9h, and the span-to-depth ratio was set to 6. The specimens were made with two different concrete grades and different steel grades as shown in Table 2. The loading process was strain-controlled before cracking and crack mouth opening displacement-controlled after cracking. The details of the steel reinforcement in Tables 3 and 4 show that the percentage was not assumed to be constant by varying the specimen size; on the contrary, it was varied by keeping the brittleness number constant N_P, defined in Eq. (6). Test results in terms of cracking loads P_{cr} and ultimate loads P_u are shown in Tables 3 and 4.

The effectiveness of the proposed model is demonstrated by a comparison between numerical predictions and experimental results for beams containing concrete grade 4 [10] in terms of applied load vs. mid-span deflection curves (Figs. 3–5). No case 4 in Table 4 is considered since each refers to a reinforcement amount considerably larger than the minimum quantity. In the numerical simulations the RC element of Fig. 2a is assumed to be representative of the mid-span portion of the beam subjected to a three-point bending test. As a result, the mid-span deflection is obtained as the sum of the localized rotation given by Eq. (11) and the elastic contribution according to the following expression:

Table 2. Material properties for the beams tested by *Bosco* et al. [10, 12]

Concrete grade	**2**			**4**			
f_{ck} (MPa)	30.0			76.0			
E_c (GPa)	23.15			34.30			
$\mathcal{G}_F$ (N/mm)	0.134			0.090			
f_{ctm} (MPa)	2.28			5.30			
	Steel used in concrete							
	Grade 2				**Grade 4**			
Φ (mm)	5	6	8	10	4	5	8	10
f_s (MPa)	673	668	704	562	680	622	675	580
f_y (MPa)	633	489	480	456	637	569	441	456

Table 3. Cracking loads P_{cr} and ultimate loads P_u for concrete grade 2 beams [12]

Case	h (mm)	b (mm)	Steel	A_s/b_wh (%)	P_{cr} (kN)	P_u (kN)
1	100	150	1ϕ5	0.131	11.26	11.49
2	100	150	2ϕ5	0.261	11.10	21.21
3	100	150	3ϕ5	0.392	11.25	29.23
1	200	150	1ϕ6	0.094	11.34	12.26
2	200	150	2ϕ6	0.188	14.05	23.35
3	200	150	3ϕ6	0.283	12.11	33.00
1	400	150	1ϕ8	0.083	19.94	23.65
2	400	150	2ϕ8	0.167	21.73	37.99
3	400	150	3ϕ8	0.250	18.75	55.94
1	800	200	1ϕ10	0.049	35.24	29.10
2	800	200	2ϕ10	0.098	43.37	44.40
3	800	200	3ϕ10	0.147	45.60	97.65

Table 4. Cracking loads P_{cr} and ultimate loads P_u for concrete grade 4 beams [10]

Case	h (mm)	b (mm)	Steel	A_s/b_wh (%)	P_{cr} (kN)	P_u (kN)
0	100	150	0	0.000	11.77	0.00
1	100	150	1ϕ4	0.085	11.77	5.78
2	100	150	2ϕ5	0.256	12.51	11.28
3	100	150	2ϕ8	0.653	13.53	22.06
4	100	150	2ϕ10	1.003	14.91	47.81
0	200	150	0	0.000	22.55	0.00
1	200	150	1ϕ5	0.064	19.53	5.80
2	200	150	3ϕ5	0.190	20.84	17.14
3	200	150	3ϕ8	0.490	22.36	56.72
4	200	150	3ϕ10	0.775	26.68	76.56
0	400	150	0	0.000	40.20	0.00
1	400	150	2ϕ4	0.043	36.67	8.40
2	400	150	4ϕ5	0.128	38.73	24.39
3	400	150	4ϕ8	0.327	43.14	65.00
4	400	150	4ϕ10	0.517	48.93	97.65

$$\delta = \delta_{loc} + \delta_{el} = \frac{\vartheta L}{4} + \frac{1}{48}\frac{PL^3}{E_c I} \tag{17}$$

where L is the beam span and I is the moment of inertia of the cross-section.

As reported in Table 2, the value of the fracture energy determined on pre-notched beams, according to the RILEM TC 50-FCM recommendation [26], is $\mathcal{G}_F$ = 0.09 N/mm. However, the value of the fracture energy adopted in the simulations in order to achieve a best fit for the experimental results refers to the beams without reinforcement (Figs. 3a, 4a, 5a) and is $\mathcal{G}_F$ = 0.18 N/mm. Such a difference is due to the fact that, unlike the notched beams considered by the RILEM recommendation, initially unnotched beams such as those tested by *Bosco* et al. [10, 12] are characterized by the development of a few microcracks around the macrocrack responsible for final collapse. This phenomenon leads to an increase in the deformation and energy dissipation, without significant effects on the cracking load, given by the propagation of the macrocrack. Therefore, the increase in the value of $\mathcal{G}_F$ permits a better description of the experimental results in terms of deformation and energy dissipation even if a single equivalent cohesive crack is considered, with negligible effects on the cracking load (the tensile strength has not been increased). The curves in Figs. 3–5 show generally good agreement between numerical and experimental results. However, it should be noted that the hypothesis of sectional localization characterizing the proposed model becomes less consistent with the real mechanical behaviour of RC beams in the case of high steel percentages. In fact, in these cases the fracture phenomenon is spread more along the beam length L, which in the present model is considered only in the elastic contribution related to the load vs. displacement response.

4 Parametric analysis and discussion

The results of an extensive numerical study carried out in order to determine a relationship between the minimum reinforcement and the mechanical and geometrical parameters of a rectangular cross-section beam are presented in this section. Eight different values of beam depth h, from 25 to 3200 mm, and five different values of concrete compressive strength f_{ck}, from 20 to 80 MPa, have been considered. All the other mechanical properties of con-

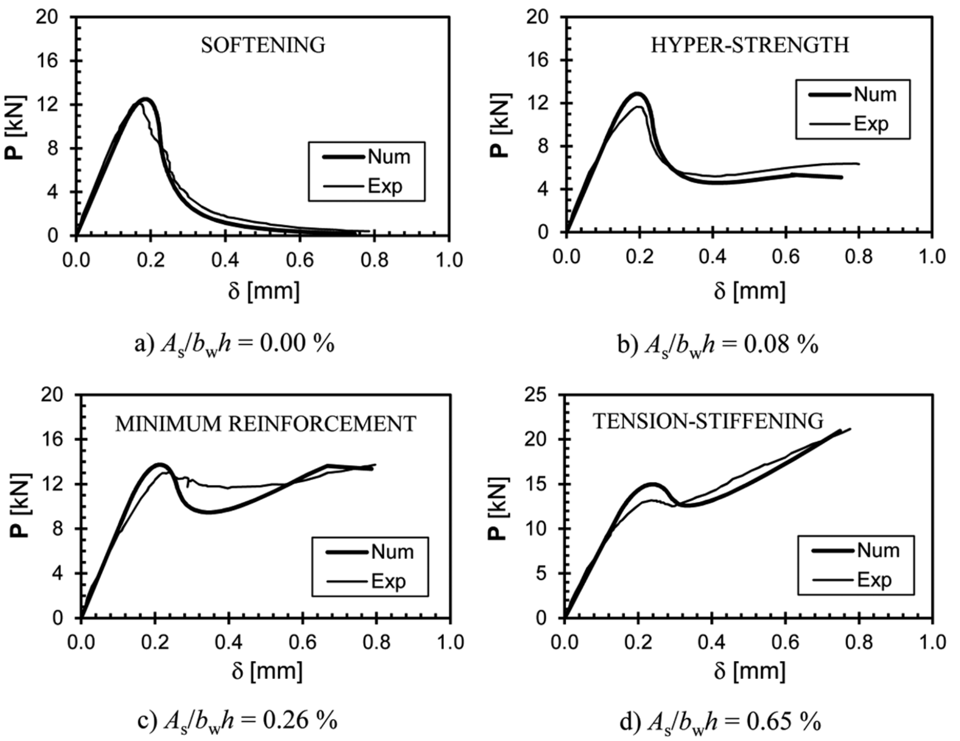

Fig. 3. Comparison between numerical and experimental [10] applied load vs. mid-span deflection curves for beam depth h = 100 mm and different amounts of tension reinforcement

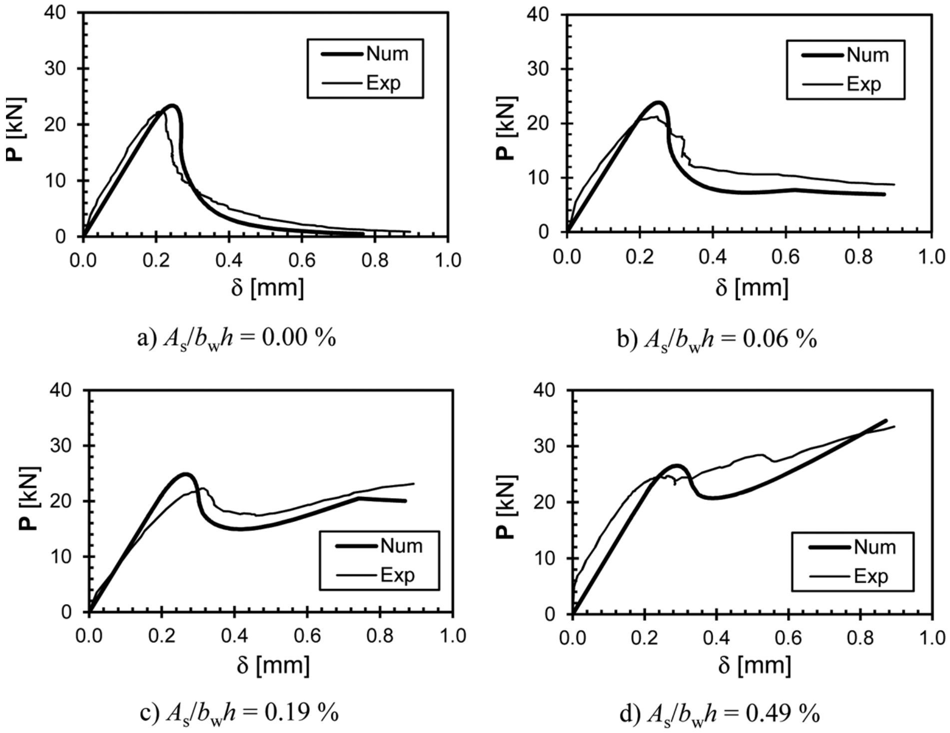

Fig. 4. Comparison between numerical and experimental [10] applied load vs. mid-span deflection curves for beam depth $h = 200$ mm and different amount of tension reinforcement

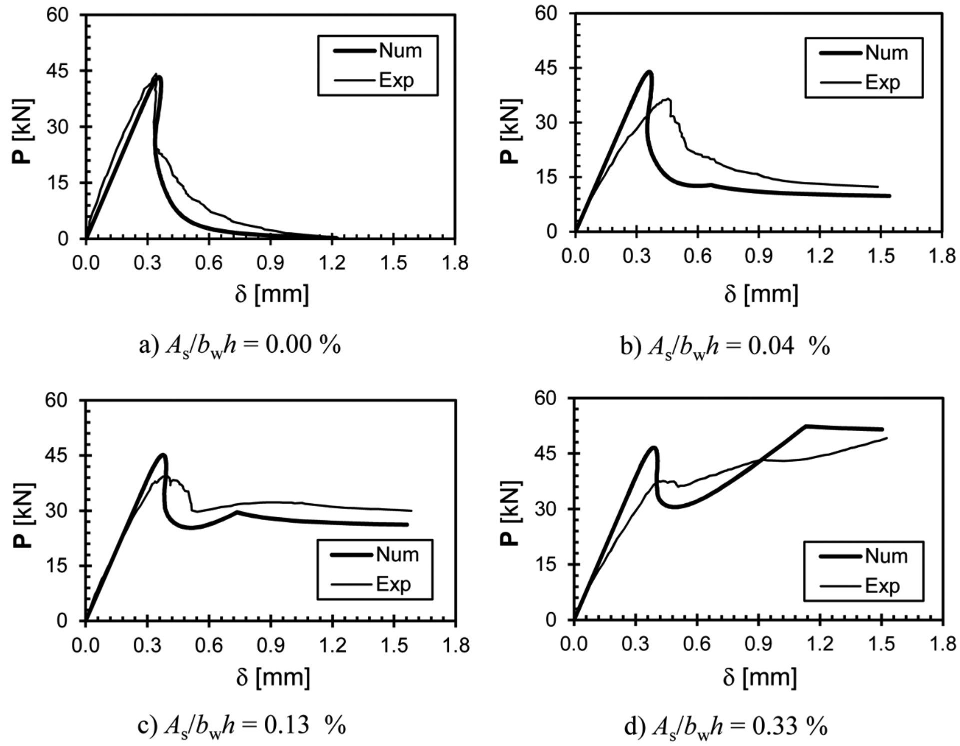

Fig. 5. Comparison between numerical and experimental [10] applied load vs. mid-span deflection curves for beam depth $h = 400$ mm and different amounts of tension reinforcement

crete have been evaluated according to the relationships provided by *fib* Model Code 2010 [2] (see Table 5). As regards the steel reinforcement, a yield strength f_{yk} = 450 MPa and an elastic modulus E_s = 200 GPa have been assumed. The ratio of effective depth to overall depth was set to 0.9. In order to find the value corresponding to the transitional mechanical response between brittle and ductile behaviour, i.e., the minimum amount from the design point of view, several simulations were carried out for each beam by varying the steel percentage. More precisely, such a transitional configuration is determined when the peak cracking load P_{cr} equals the ultimate load P_u (see

Table 5. Mechanical parameters for the rectangular beams considered in the numerical simulations

f_{ck} (MPa)	f_{ctm} (MPa)	$\mathcal{G}_F$ (N/mm)	E_c (GPa)	h (mm)	A_s/b_wh (%)	N_{PC}	s
20	2.2	0.062	30	25	0.195	0.104	3.921
				50	0.172	0.127	2.772
				100	0.157	0.164	1.960
				200	0.140	0.207	1.386
				400	0.124	0.259	0.980
				800	0.112	0.331	0.693
				1600	0.100	0.417	0.490
				3200	0.095	0.561	0.347
35	3.2	0.083	34	25	0.278	0.121	3.320
				50	0.25	0.150	2.348
				100	0.215	0.182	1.660
				200	0.193	0.231	1.174
				400	0.175	0.296	0.830
				800	0.159	0.381	0.587
				1600	0.143	0.485	0.415
				3200	0.139	0.666	0.293
50	4.1	0.103	37	25	0.350	0.129	3.011
				50	0.300	0.155	2.129
				100	0.266	0.194	1.506
				200	0.242	0.249	1.065
				400	0.220	0.321	0.753
				800	0.200	0.412	0.532
				1600	0.183	0.534	0.376
				3200	0.173	0.713	0.266
65	4.5	0.120	40	25	0.385	0.130	3.079
				50	0.335	0.154	2.177
				100	0.305	0.198	1.540
				200	0.280	0.257	1.089
				400	0.245	0.318	0.770
				800	0.220	0.404	0.544
				1600	0.197	0.512	0.385
				3200	0.192	0.705	0.272
80	4.8	0.137	42	25	0.42	0.128	3.161
				50	0.370	0.155	2.235
				100	0.332	0.197	1.580
				200	0.295	0.247	1.117
				400	0.260	0.308	0.790
				800	0.236	0.396	0.559
				1600	0.214	0.508	0.395
				3200	0.210	0.705	0.279

Fig. 6). The $A_{s,min}/b_wh$ ratios obtained for the beams considered, and the corresponding values of s and N_P (in this case N_{PC} since it contains the critical value of the reinforcement area), are reported in Table 5. The results of N_{PC} vs. s are also shown in Fig. 6, where a decrease in the critical value of the reinforcement brittleness number is seen as the stress brittleness number increases. In the range of interest for common structural applications, the trend obtained can be described with a very good approximation by the following hyperbolic curve:

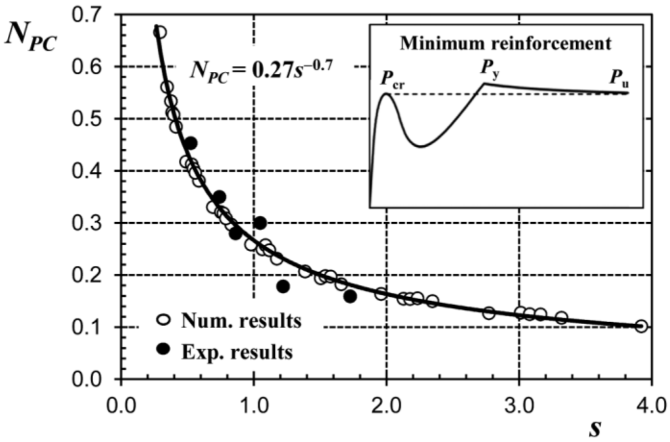

Fig. 6. Best-fit relationship of numerical results (○ symbols) between N_{PC} and s; • symbols are experimental results [10, 12]

$$N_{PC} = 0.27s^{-0.70} \tag{18}$$

By substituting Eqs. (6) and (16) in (18), the relation for the minimum reinforcement area reads as follows:

$$A_{s,min} = 0.27\frac{(f_{ctm})^{0.70}(K_{IC})^{0.30}}{f_{yk}}b_w h^{0.85} \tag{19}$$

According to Eq. (19), $A_{s,min}$ is an increasing function of the tensile strength and toughness of concrete, and of the width and depth of the beam, whereas it is a decreasing function of the steel yield strength. The minimum reinforcement amount derived by the experimental tests of *Bosco* et al. [10, 12] for concrete grades 2 and 4 are indicated in Fig. 6 by the • symbols. The values – in some cases obtained by interpolating the data reported in Tables 3 and 4 – confirm the trend of the numerical results. The same calculations have also been performed for a T-beam with the flange in compression having a width $8b_w$ and depth $0.20h$. Such geometrical ratios determine a section modulus 1.5 times larger than that of a rectangular section having the same depth and a width b_w (the same case considered by ACI 318 [4]). The expression obtained for the minimum reinforcement area is

$$A_{s,min} = 0.34\frac{(f_{ctm})^{0.84}(K_{IC})^{0.16}}{f_{yk}}b_w h^{0.92} \tag{20}$$

The minimum reinforcement percentages $\rho_{min} = A_{s,min}/b_wd$ obtained from Eqs. (19) and (20) are compared with the prescriptions of the design codes [2, 4, 6, 7] in Fig. 7 for f_{ck} = 35 MPa, and f_{yk} = 450 MPa. The reinforcement ratio given by the Norwegian Standard is slightly larger than that given by Eq. (19) for any beam depth. The provisions of Eurocode 2 and *fib* Model Code 2010 are unsafe for beam depths < 540 mm, whereas they overestimate the reinforcement ratio for d > 540 mm. It is worth noting that, for the same value of d/h and for a resistance factor equal to unity, the curve proposed for rectangular beams (Eq. (19)) should tend to the provisions of Eurocode 2 and *fib* Model Code 2010 for large beam depths, i.e. when the cohesive forces can be neglected. As regards the ACI 318-08 provision, it is considerably higher than the curve pro-

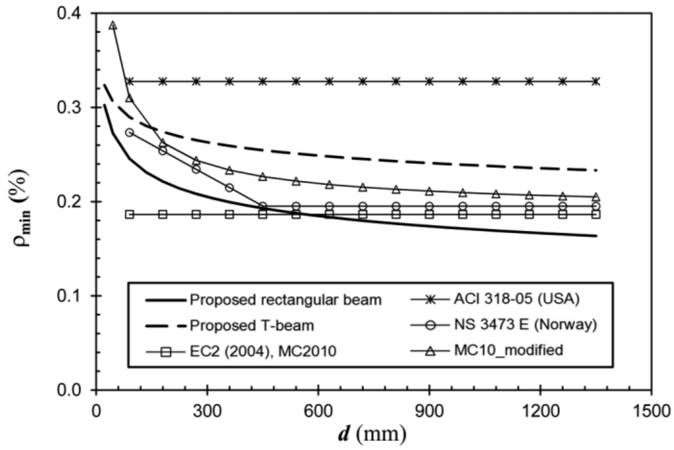

Fig. 7. Comparison of minimum reinforcement ratios calculated by different codes [2, 4, 6, 7] for $f_{yk} = 450$ MPa and $f_{ck} = 35$ MPa

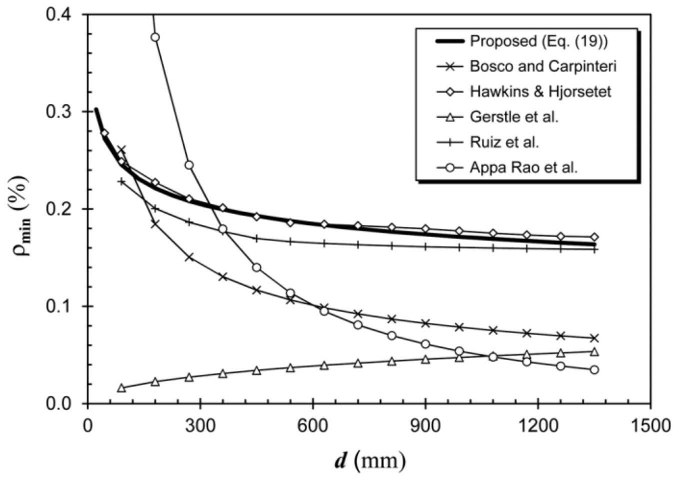

Fig. 8. Minimum reinforcement vs. effective beam depth according to various models [11–15] for $f_{yk} = 450$ MPa and $f_{ck} = 35$ MPa

posed for T-beams (Eq. (20)). In this case too, the proposed curve does not tend to the ACI provision for large beam depths due to a different value for the d/h ratio and the application of the resistance factor. Furthermore, in the ACI approach the flexural tensile strength is adopted for concrete instead of the direct tensile strength used in the cohesive model. According to the American standard, the flexural strength is greater than the direct tensile strength and is independent of size, whereas it is actually a decreasing function of the beam depth. This assumption results in a greater overestimation of the minimum reinforcement for large beam depths. Finally, the curve in Fig. 7 labelled "MC10-modified" is obtained by substituting the uniaxial tensile strength of concrete f_{ctm} in Eq. (4) by the flexural tensile strength $f_{ct,fl}$ which, according to *fib* Model Code 2010, is given by

$$f_{ct,fl} = f_{ctm} \frac{(1 + 0.06h^{0.7})}{0.06h^{0.7}} \tag{21}$$

The shape of the curve obtained is very similar to the proposed one, even if it overestimates the minimum reinforcement. This is due to the fact that the coefficient 0.26 in Eq. (4) includes a resistance factor, as specified in section 1.1. In case a unitary resistance factor is considered, the proposed curve for rectangular cross-sections and the *fib* Model Code 2010 modified prescription would be almost coincident.

The minimum reinforcement percentage vs. beam depth curves according to the different models available in the literature (see Table 1) are compared with Eq. (19) in Fig. 8 for $f_{ck} = 35$ MPa and $f_{yk} = 450$ MPa. The effective beam depth has been kept at $0.9h$ at any scale. The model by *Gerstle* et al. [13] presents an increase in the minimum steel percentage as the beam depth increases. All the other curves clearly highlight a decreasing trend. The proposed curve is very close to those related to the studies by *Hawkins* and *Hjorsetet* [12] and *Ruiz* et al. [14], also based on the cohesive crack model. It should be noted, however, that the application of dimensional analysis permits better clarification of the effects of each of the variables involved in the physical phenomenon, as well as their interaction in the global response, for both rectangular and T-beams. Contrary to the bridged crack model, the proposed approach can be applied to unreinforced concrete beams too. When $N_P = 0$ due to $A_s = 0$, the overall mechanical behaviour is in fact a function of the dimensionless number s. Small values for beam depths mean high values for s and therefore a ductile response.

For the sake of completeness, it should be remarked that Eqs. (19) and (20) can only be applied within the range of beam depths considered in the present study. Their asymptotes for a beam depth tending to zero and to infinity are in fact incorrect. For h tending to zero, the minimum reinforcement ratio is approximately equal to $(f_{ctm}\ h^2)/(2f_{yk}\ d^2)$ since very small beams fail in a ductile manner, and the closing tractions along the cohesive crack can be assumed constant, even for large rotational hinges. On the other hand, for h tending to infinity, ρ_{min} is equal to $(f_{ctm}\ h^2)/(6f_{yk}\ d^2)$ for rectangular sections and $(f_{ctm}\ h^2)/(4f_{yk}\ d^2)$ for the T-section considered due to the fact that the cohesive contribution can be neglected.

5 Summary and conclusions

New formulae for evaluating the minimum reinforcement have been derived by applying dimensional analysis to the results of a numerical algorithm proposed to study the flexural behaviour of lightly reinforced RC beams with rectangular and T-shaped sections. Such an approach permits the main mechanical and geometrical parameters affecting the phenomenon being studied – namely the concrete fracture toughness and tensile strength, the steel yield strength and the structural size – to be considered by means of two dimensionless numbers, N_P and s. Other effects, such as the steel-concrete interaction, the size and spacing of the rebars and the concrete cover, have not been analysed in the present study since they affect the dependence of the minimum reinforcement amount on the beam dimensions only marginally. As far as size-scale effects are concerned, it should be noted that the presence of cohesive closing stresses determines a variation in ρ_{min} with the beam size which is less pronounced than that predicted by the bridged crack model. It turns out to be a function of $h^{-0.15}$ for rectangular beams and $h^{-0.08}$ for T-beams, instead of the $h^{-0.50}$ obtained by LEFM. Such a difference is clearly shown in Fig. 8, where the curve of *Bosco* and *Carpinteri* [11] is compared with the present proposal. The proposed formulae, Eqs. (19) and (20), can be further rearranged for practical purposes by expressing f_{ctm} and K_{IC} as functions of f_{ck} according to relationships available in the literature and/or in design codes (see, for example, *fib* Model Code 2010 [2]). Alternatively, very similar results can be obtained by applying the prescription provided by Eurocode 2 and *fib* Model Code 2010 (Eq. (4)), in which the uniaxial tensile strength is replaced with the flexural tensile strength given by Eq. (21). The formula obtained is certainly suitable for practical purposes.

Finally, it should be remarked that, in order to tackle the problem of minimum reinforcement fully, the serviceability conditions should also be studied accurately. According to the approach of *fib* Model Code 2010, for instance, more restrictive prescriptions for the minimum amount of reinforcement may be derived from limitations to the crack mouth opening displacement necessary to prevent steel corrosion and improve durability. Size effects are also expected to influence the crack opening in this case, and therefore the minimum reinforcement, as revealed in experiments by *Yasir Alam* et al. [27].

Acknowledgements

The financial support provided by the Ministry of University and Scientific Research (MIUR) for the project "Advanced applications of Fracture Mechanics for the study of integrity and durability of materials and structures" is gratefully acknowledged.

Notation

A_c	gross cross-sectional area
A_s	steel reinforcement area
b_w	width of tension side of beam
d	effective depth of beam
D_M	coefficient of influence for applied moment
$\{D_w\}^T$	vector of coefficients of influence for nodal displacements
E_c	elastic modulus of concrete
E_s	elastic modulus of steel
f_{ck}	characteristic compressive strength of concrete
f_{cm}	average compressive strength of concrete
f_{ctm}	average uniaxial tensile strength of concrete
$f_{ct,fl}$	flexural tensile strength of concrete
f_{yk}	characteristic tensile yield strength of steel
$\{F\}$	vector of nodal forces
$\mathcal{G}_C$	crushing energy of concrete
$\mathcal{G}_F$	fracture energy of concrete
h	overall depth of beam
K_{IC}	concrete fracture toughness
$\{K_M\}$	vector of coefficients of influence for applied moment
$[K_w]$	matrix of coefficients of influence for nodal displacements
L	span of beam
l	length of beam portion considered
M	applied bending moment
M_u	nominal flexural resistance (reaction of yielded reinforcement x moment arm)
M_{cr}	cracking moment of plain concrete section
N_P	reinforcement brittleness number
N_{PC}	critical value for reinforcement brittleness number, corresponding to minimum reinforcement amount
P	applied load
P_{cr}	maximum cracking load
P_u	ultimate load with respect to yielded steel and completely cracked cross-section
s	stress brittleness number
$\{w\}$	vector of nodal displacements
w_{cr}^c	critical overlapping displacement
w_{cr}^t	critical crack opening displacement
δ	mid-span deflection
ϑ	localized rotation of beam portion considered
ρ	$(A_s/b_w d) \times 100$, steel reinforcement percentage
ϕ	resistance factor

References

1. *Balázs, G. L.*: Design for SLS according to *fib* Model Code 2010. Structural Concrete, 2013, 14, No. 2, pp. 99–123.
2. Federation International du Beton (ed.): Model Code 2010 – First complete draft, vol. 1, Thomas Telford Ltd, Lausanne, *fib* Bulletin No. 55, 2010.
3. American Concrete Institute Committee 318 (ed.): Building Code Requirements for Structural Concrete (ACI 318-95) and Commentary (ACI 318R-95), Detroit, MI, 1995.
4. American Concrete Institute Committee 318 (ed.): Building Code Requirements for Structural Concrete (ACI 318-08) and Commentary (ACI 318R-08), Farmington Hills, MI, 2008.
5. *Seguirant, S. J., Brice, R., Khaleghi, B.*: Making sense of minimum flexural reinforcement requirements for reinforced concrete members. PCI Journal, 2010, 55, No. 3, pp. 64–85.
6. European Committee for Standardization (ed.): Eurocode 2: Design of Concrete Structures, Part 1-1: General Rules and Rules for Buildings, Brussels, 2004.
7. Norwegian Standard, NS 3473 E (English translation): Concrete Structures, Design Rules, Norwegian Council for Building Standardization, Olso, Norway, 1989.
8. *Carpinteri, A.*: Stability of fracturing process in RC beams. Journal of Structural Engineering, 1984, 110, No. 3, pp. 544–558.
9. *Bosco, C., Carpinteri, A.*: Softening and snap-through behavior of reinforced elements. Journal of Engineering Mechanics, 1992, 118, No. 8, pp. 1564–1577.
10. *Bosco, C., Carpinteri, A., Debernardi, P. G.*: Minimum reinforcement in high-strength concrete. Journal of Structural Engineering, 1990, 116, No. 2, pp. 427–437.
11. *Bosco, C., Carpinteri, A.*: Fracture mechanics evaluation of minimum reinforcement in concrete structures. In: Applications of Fracture Mechanics to Reinforced Concrete, *Carpinteri, A.* (ed.), Elsevier Applied Science, London, 1992, pp. 347–377.
12. *Hawkins, N. M., Hjorsetet, K.*: Minimum reinforcement requirements for concrete flexural members. In: Applications of Fracture Mechanics to Reinforced Concrete, *Carpinteri, A.* (ed.), Elsevier Applied Science, London, 1992, pp. 379–412.
13. *Gerstle, W. H., Dey, P. P., Prasad, N. N. V., Rahulkumar, P., Xie, M.*: Crack growth in flexural members – a fracture me-

chanics approach. ACI Structural Journal, 1992, 89, No. 6, pp. 617–625.
14. *Ruiz, G., Elices, M., Planas J.*: Size effects and bond-slip dependence of lightly reinforced concrete beams. In: Minimum Reinforcement in Concrete Members, *Carpinteri, A.* (ed.), Elsevier Science Ltd., Oxford, UK, 1999, pp. 127–180.
15. *Appa Rao, G., Aravind, J., Eligehausen, R.*: Evaluation of minimum flexural reinforcement in rc beams using fictitious crack approach. Journal of Structural Engineering (Madras), 2007, 34, No. 4, pp. 277–283.
16. *Jenq, Y. S., Shah, S. P.*: Shear resistance of reinforced concrete beams – a fracture mechanics approach. In: Fracture Mechanics: Application to Concrete (special report ACI SP-118), *Li, V. C., Bazant, Z. P.* (eds.), American Concrete Institute, Detroit, 1989, pp. 327–358.
17. *Carpinteri, A., Corrado, M., Mancini, G., Paggi, M.*: Size-scale effects on plastic rotational capacity of rc beams. ACI Structural Journal, 2009, 106, No. 6, pp. 887–896.
18. *Carpinteri, A.*: Size effects on strength, toughness and ductility. Journal of Engineering Mechanics, 1989, 115, pp. 1375–1392.
19. *Planas, J., Elices, M.*: Asymptotic analysis of a cohesive crack: 1. theoretical background. International Journal of Fracture, 1992, 55, No. 2, pp. 153–177.
20. *Hillerborg, A., Modeer, M., Petersson, P. E.*: Analysis of crack formation and crack growth in concrete by means of fracture mechanics and finite elements. Cement and Concrete Research, 1976, 6, pp. 773–782.
21. *Carpinteri, A., Corrado, M., Mancini, G., Paggi, M.*: The overlapping crack model for uniaxial and eccentric concrete compression tests. Magazine of Concrete Research, 2009, 61, No. 9, pp. 745–757.
22. *Tammo, K., Thelandersson, S.*: Crack widths near reinforcement bars for beams in bending. Structural Concrete, 2009, 10, No. 1, pp. 27–34.
23. *Buckingham, E.*: Model experiments and the form of empirical equations. ASME Transaction, 1915, 37, pp. 263–296.
24. *Carpinteri, A.*: Notch sensitivity in fracture testing of aggregative materials. Engineering Fracture Mechanics, 1982, 16, No. 4, pp. 467–481.
25. *Corrado, M., Cadamuro, E., Carpinteri, A.*: Dimensional analysis approach to study snap back-to-softening-to-ductile transitions in lightly reinforced quasi brittle materials. International Journal of Fracture, 2011, 172, pp. 53–63.
26. RILEM TC 50-FCM: Determination of the fracture energy of mortar and concrete by means of three-point bend tests on notched beams. Materials and Structures, 1985, 18, pp. 285–290.
27. *Yasir Alam, S., Lenormand, T., Loukili, A., Regoin, J. P.*: Measuring crack width and spacing in reinforced concrete members. Proc. of FraMCoS-7, *Oh, B. H.* (ed.), Korea Concrete Institute, Seoul, 2010, pp. 377–382.

Prof. Alberto Carpinteri
Department of Structural
Geotechnical and Building Engineering
Politecnico di Torino
Corso Duca degli Abruzzi, 24
10129 Torino, Italy

Dr. Erica Cadamuro
Department of Structural
Geotechnical and Building Engineering
Politecnico di Torino
Corso Duca degli Abruzzi, 24
10129 Torino, Italy

Dr. Mauro Corrado
Corresponding author
Department of Structural
Geotechnical and Building Engineering
Politecnico di Torino
Corso Duca degli Abruzzi, 24
10129 Torino, Italy
Tel. +39 011 0904858
Fax +39 011 0904899
E-mail: mauro.corrado@polito.it